

# Evaluation of Camera Calibration Methods for Star Identification (December 2007)

Pedro Davalos

**Abstract**—Star Navigation is one of the oldest methods used for navigation as stars provide a reliable independent source of valuable information that translates to position and heading information. Although manual star navigation is slowly being replaced by modern navigation systems such as Global Positioning System (GPS), stars still provide the same reliable navigation information as they did centuries ago. Since the 1960's, the aviation and aerospace industries has been researching and developing autonomous star trackers capable of imaging the night-sky with a camera or imaging device, and then process the images to extract star locations. This paper focuses on camera calibration intended for autonomous star trackers, by evaluating various calibration methods including a calibration technique for cameras on-board deployed spacecrafts. The calibration is evaluated by applying the relationship of the law of cosines that define the angle between two vectors and the pinhole projectivity camera model as we have known angles between stars and their corresponding star centroids (locations of pixel coordinates) on the image.

**Index Terms**— Camera Calibration, Inter-star Angles, Star Identification, Star Navigation, Star Tracker

## I. INTRODUCTION

THIS document presents a systematic evaluation of four different camera calibration techniques: 1) 2d-3d point correspondence, 2) homographies from three planes, 3) a Numerical Method that solves the non-linear system established by the law of cosines relationship between points/vectors/angles, and 4) a third party Toolbox implemented by Jean-Yves Bouguet [1] based on Zhang's Calibration Method [2] with added optimizations.

Each of the four calibration techniques is verified by the law of cosines equation that defines the relationship between points, vectors, and angles for a pinhole camera model, where we have known angles, obtained from inter-star angles and we can compare these know angles with its corresponding imaged stars.

Our results will serve as an indicator of the sensitivity to

various parameters affecting the output, such as relative magnitude of the inter-star angle, star centroids extracted from the image, and sensitivities from calibration itself. However, we expect to obtain accurate inter-star angle estimates for all calibration techniques, with small bias and small variance from the error distribution.

Star Identification is the process of recognizing with certainty each star in a given image, Star Trackers need to automatically identify stars in a given image much like a human observer can identify star constellations in the night sky. However, Star Trackers have a limited fixed field of view (FOV). The process of recognizing stars from a single image without any prior knowledge about the direction of the FOV is usually referred to as the Lost In Space Algorithm (LISA).

Automated star identification is a challenging task as imaged stars appear as identical "dots" where the only distinguishable feature is the relative brightness, or the size of the "dot". Consequently star identification usually consists of pattern matching based on triangles formed by stars.

Star Tracker implementations require a broad range of disciplines including astronomy, orbital mechanics, and various fields in computer science such as algorithms analysis for optimizing searches and pattern matching as well as computer vision. However, this study focuses on the estimation of inter-star angles, which is a critical component of Star Trackers regardless of the pattern matching search technique used for star identification.

## II. RELATED WORK

Star Trackers for attitude estimation and navigation is an extensively researched topic in the aerospace industry, and due to the high level of complexity from the multiple subcomponents involved with star trackers, each sub-component is a challenging independent problem that has been optimized. For instance, star catalog databases require astronomy for optimizing the minimum number of stars that fit a given Field Of View, or identify the Field of View that would optimize the Star Catalog by selecting the brightness threshold that would guarantee a minimum number of bright stars in any given view of the night sky [3][4][5].

Once the star catalog has been identified, including the establishment of an accessible coordinate system, camera

Manuscript received December 1, 2007. This work was supported in part by the Departments of Computer Science and Aerospace Engineering at Texas A&M University in conjunction with the Spacecraft Technology Center of the Texas Engineering Experiment Station (TEES).

P. Davalos is with Texas A&M University, College Station, TX 77843 USA (phone: 979-845-8768; e-mail: pedro@tamu.edu).

calibration must be performed in order to find the lens distortion model and to find the intrinsic parameters of the camera including the focal length and the principal point. Camera calibration is a critical part for star trackers since the primary objective is to perform accurate measurements of the 3-dimensional world, specifically finding angles between rays from the center of the camera, to the stars assumed to be at a plane at infinity. In addition, research has been conducted to analyze calibration techniques for deployed cameras onboard spacecrafts [6], and the effects of star identification have also been analyzed if camera calibration was unavailable [7].

Another basic Star Tracker task is to process the image to extract stars from the image. This process is known as “star centroiding,” as it involves preprocessing the image to find the distribution of the pixel intensities of the background, find any invalid pixels, and find a threshold that distinguishes stars from the background. The size of imaged stars varies depending on the Field of View and the number of pixels on the imager sensor, and the size could range from 2x2 pixels and 40x40 pixels, regardless of the size of each star, the exact location of the center can be estimated by using standard density estimation techniques such as Maximum Likelihood Estimate known also as Center of Mass estimation, since each star is usually shaped like a 2-dimensional Gaussian distribution [8][9].

Furthermore, Star Trackers must perform pattern matching to find the given star pattern from an image on the star catalog which contains the entire sky, and once the star pattern is found, accurate attitude information can be obtained [10]-[14].

However, since this study specializes in the effect of calibration, it can be compared with previous work by Andreas Klaus *et al.* [15], where similar research was conducted with the purpose of extracting calibration parameters by inspecting known star pairs with known inter-star angles. Which is exactly our motivation for our third calibration technique of reverse calibration.

### III. CALIBRATION TECHNIQUES

During this study, we evaluated four different camera calibration techniques. Where the goal of calibrating the camera is to find the intrinsic parameters that define the camera model.

The pinhole camera model defines the projections of the 3-dimensional real world onto the 2-dimensional image. Since this study focuses on cameras for star trackers, and stars can be considered to be points at infinity, the “ray” from the camera’s center to the star passes through its imaged location for each star in the Field Of View (FOV). Consequently we can measure the angle between any pair of imaged stars by the law of cosines between the two rays for each star, and the intrinsic parameters from a calibrated camera allows for us to accurately measure that inter-star

angle. Star projections onto images is illustrated on Fig. 1,

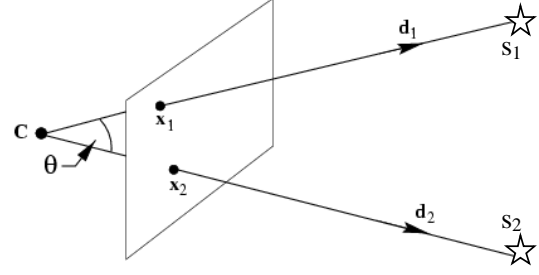


Fig. 1. Inter-Star angles  $\theta$ , can be found by calibrated camera with known camera center (C) as the angle between stars  $s_1$  and  $s_2$ , where  $x_1$  and  $x_2$  are the location of the stars on the image. An imaged star  $x_i$  is the intersection of the image plane and the ray from the camera center (C) and the star  $s_i$

and the angle between the two rays from the camera center (C) to the stars can be found as described in (1).

$$\cos \theta = \frac{d_1^T d_2}{\sqrt{(d_1^T d_1)(d_2^T d_2)}} = \frac{x_1^T (K^{-T} K^{-1}) x_2}{\sqrt{(x_1^T (K^{-T} K^{-1}) x_1)(x_2^T (K^{-T} K^{-1}) x_2)}} \quad (1)$$

The camera calibration matrix  $K$  in (1) is a 3x3 uptriangular matrix that contains the intrinsic calibration parameters: focal length ( $f$ ), principal point ( $x_o, y_o$ ), skew coefficient ( $s$ ), and the pixel aspect ratio ( $m_x, m_y$ ). The composition of the  $K$  matrix is shown on (2).

$$K = \begin{bmatrix} f \cdot m_x & s & x_o \\ 0 & f \cdot m_y & y_o \\ 0 & 0 & 1 \end{bmatrix} \quad (2)$$

Once the intrinsic calibration parameters ( $K$ ) are found, the metric we will use to evaluate each calibration technique is the difference between true angles and estimated angles. Where true angles will be obtained from the star catalog, and estimated angles will be found by applying (1) with the corresponding imaged stars ( $x_1, x_2$ ) and the calibration parameters ( $K$ ).

#### A. 2D-3D Correspondence

Obtaining camera calibration from the correspondence of 2-dimensional points and 3-dimensional points can be accomplished by applying the basic properties of image projections. 3D points ( $X$ ) are projected to the 2D image coordinates ( $x$ ) by the camera projection matrix  $P$  as defined in (3), where matrix  $P$  is a 3x4 matrix.

$$x = P \cdot X \quad (3)$$

From this relationship we can solve for  $P$  by rearranging the equation as described in (4), where  $P^i$  is a 4-vector containing the  $i^{\text{th}}$  row of matrix  $P$

$$\begin{bmatrix} \mathbf{0}^T & -w_i X_i^T & y_i X_i^T \\ w_i X_i^T & \mathbf{0}^T & -x_i X_i^T \end{bmatrix} \begin{pmatrix} P^1 \\ P^2 \\ P^3 \end{pmatrix} = \mathbf{0} \quad (4)$$

Once we find the camera matrix  $P$ , we can decompose  $P$  through RQ decomposition of the first 3x3 submatrix of  $P$  to

find the intrinsic calibration matrix  $K$ . This calibration process is further described in [16].

### B. Three Planes

Calibration from imaging three planes can be obtained by finding the homographies that project each imaged plane to the image plane. These three planes could be squared surfaces at different orientations, where each homography obtained from each plane can provide two circular points on the image of the absolute conic (IAC),  $\omega$ . Since each homography provides two points on the conic  $\omega$ , we can solve for  $\omega$  with 3 homographies (3 planes). If each homography  $H$ , is composed of columns  $[h_1, h_2, h_3]$ , the  $3 \times 3$  matrix  $\omega$  can be found from at least 3 planes, since each homography allows for two equations (5) and (6) that correspond to the real and imaginary parts of the circular points. Additional information can be found on [2], and pp. 209-212 of [16].

$$h_1^T \cdot \omega \cdot h_2 = 0 \quad (5), (6)$$

$$h_1^T \cdot \omega \cdot h_1 = h_2^T \cdot \omega \cdot h_2$$

Since  $\omega$  equals  $K^{-T} K^{-1}$ , we do not need to explicitly find  $K$  when only working with angle estimation. However, the conic  $\omega$  can be decomposed to find  $K$  through cholesky's decomposition [16] or through Zhang's method [2].

### C. Reverse

Camera calibration is usually performed through computation of the image of the absolute conic [2], through the plane at infinity and vanishing points [16], or through 2D-3D correspondence [16] as described earlier, before any engineering measurements such as angles are extracted from images. However, the reverse calibration method can be accomplished if accurate angles are known for corresponding imaged points, which is the case when imaging a known portion of the sky with labeled stars in the field of view. Each pair of stars with it's corresponding inter-star angle provides all information required for (1), except the calibration parameters. Therefore, we can utilize the multiple star pairs in a single image to generate an overdetermined system that can be solved through non-linear numerical methods such as Leavenberg-Marquardt or Newton-Gauss to solve for the Image of the Absolute Conic (IAC),  $\omega$ . That can be decomposed into the camera calibration parameters  $K$  as described earlier.

This reverse calibration method has an extraordinary potential for calibrating cameras onboard deployed spacecrafts if original ground calibration is unavailable or to recalibrate the camera to compensate for any hardware reconfigurations experienced during launch, or to compensate for hardware deformations due to thermal cycles and material fatigue. Consequently, the reverse calibration method has been previously researched for this same purpose [15] [6].

### D. J. Bougette Matlab Toolbox Benchmark [1]

The fourth camera calibration method we will evaluate is a software package developed by Jean-Yves Bougette [1], which is compiled as a Matlab Toolbox. This Toolbox is based on Zhang's calibration method [2] of imaging multiple planes, then finding the conic that fits the circular points from the homographies. This package performs optimizations at multiple stages of the process, which is why we would expect superior performance through this method than by our previous basic implementations. Furthermore, the skew calibration parameter is enforced to zero, which is a reasonable assumption for this study.

## IV. RESULTS

As previously discussed, the criteria we will use to evaluate each of the four calibration techniques is the difference between the true angles and the estimated angles between star pairs. The true angles are obtained from the star catalog, and estimated angles will be obtained from applying (1) to the imaged star points and the calibration parameters,  $K$ .

### A. Results from 2D-3D Correspondence

After applying the correspondence from (4), on the selected 2D points the image (Fig. 2), and the 3D points as measured, with the camera center as the origin (Fig. 3), we obtain the  $K$  camera calibration matrix:

$$K = \begin{bmatrix} 2955 & -7 & 1310 \\ 0 & 2947 & 926 \\ 0 & 0 & 1 \end{bmatrix}$$

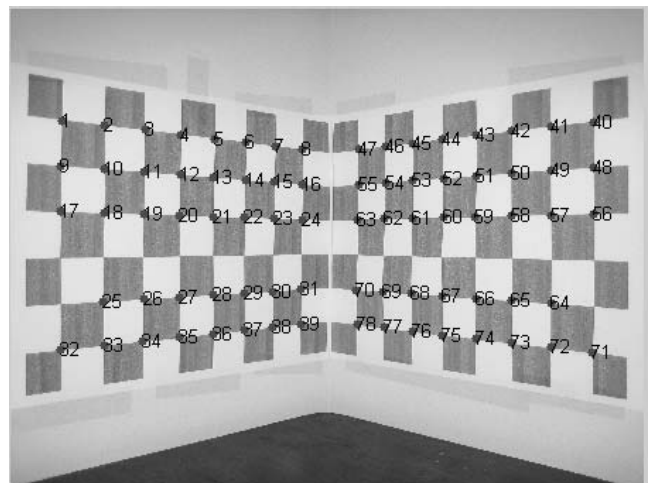


Fig. 2. Image of calibration sheet for 2D-3D correspondence, with selected points overlaid as red dots labeled with their corresponding index label.

Finally, after computing the difference between true angles and estimated angles, we obtain the error distribution as shown on Fig. 4, where the mean error is 1.37 degrees.

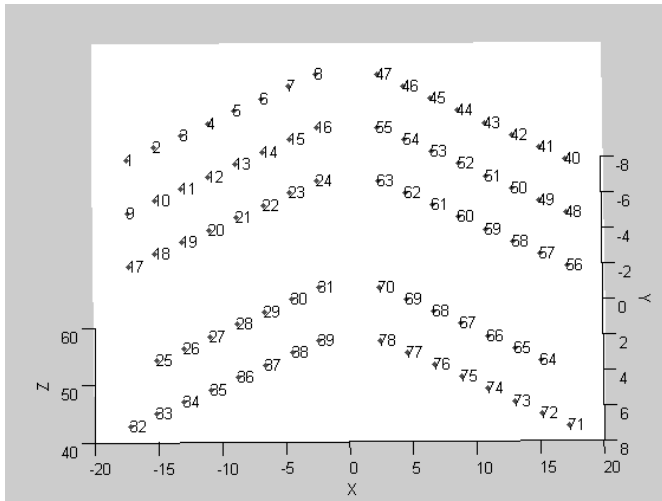


Fig. 3. 3D points as measured with the camera center at the origin, corresponding to the imaged points illustrated on Fig. 2.

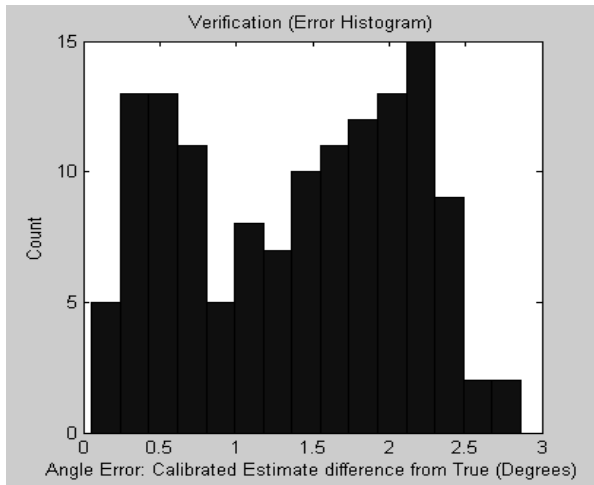


Fig. 4. Error distribution from the difference of true inter-star angles and estimated angles using 2D-3D correspondence calibration.

**B. Results from Calibration through 3 Planes**

Calibration from three planes can be accomplished by computing the homography that projects the given plane to the imager plane. These projections require knowledge from the image to project to a similarity where parallel lines are parallel, which is why rectangular shapes are used to define the planes. However, we analyzed 3 different methods to accomplish this calibration technique, the first method we used rectangles as shown in Fig. 5a. The second method consisted of representing planes by squares (Fig 5b), and finally, the third method using three distinct images of a plane from different camera locations (Fig. 6).

After computing the Homographies and the circular points, calibration is established by fitting the conic through the circular points, where we obtain three different calibrations

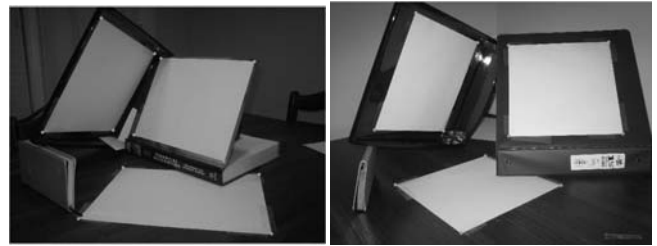


Fig. 5. Calibration Image containing three planes. (a) Using rectangles (left), and (b) using squares (right).



Fig. 6. Images for camera calibration from 3-planes, where each plane is located on separate images.

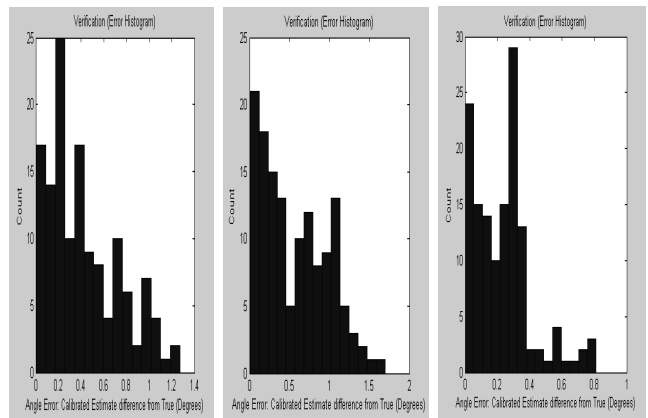


Fig. 7. Error Distributions from calibration through 3 planes (a) using rectangles (left), (b) using squares (middle), and (c) using three images (right).

since we used three different methods using this same technique.

The results are presented in Fig. 7, where the error distribution is the difference between the true inter-star angle and the estimated inter-star angle by applying (1) to each star pair in our night sky image. The average error is  $.42^\circ$  using rectangles,  $.57^\circ$  using squares, and  $.23^\circ$  using three images.

**C. Results from Reverse Calibration**

Reverse calibration, as previously defined, is the process of extracting the calibration parameters from a single image with known inter-star angles between imaged star pairs, since this information provides all parameters in (1) except the calibration parameters,  $K$ .

Implementation of the reverse calibration was accomplished by Matlab's built-in function `lsqnonlin`, which performs the non-linear least squares fitting using the results from the previous technique (three-planes from three separate

images) for initialization.

Results from reverse calibration are shown on Fig. 8, where the error distribution illustrates the difference between the true inter-star angles, and the estimated inter-star angles using the calibration parameters,  $K$ , found from reverse calibration. The average error was found to be 0.25 degrees.

*D. Results from calibration using the Matlab Toolbox [1]*

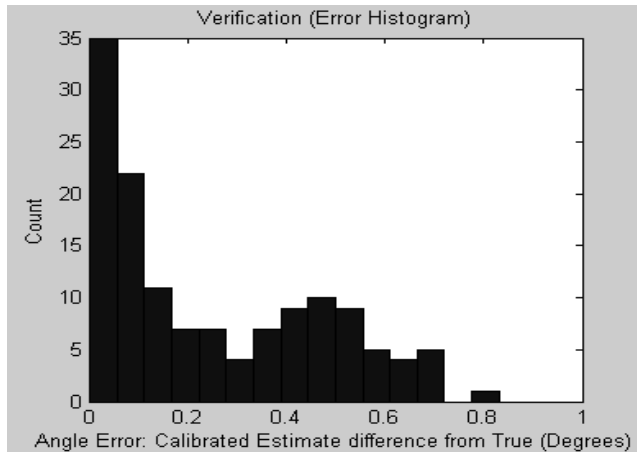


Fig. 8. Error distribution from the difference of true inter-star angles and estimated angles using reverse calibration.

Jean-Yves Bouguet’s camera calibration toolbox [1], is an optimized camera calibration package based on Zhang’s calibration technique [2]. Consequently, because of these optimizations, we expect superior performance through this calibration implementation.

The calibration experiment consisted of 13 input images of the calibration pattern each taken at a different viewpoint. Which translates to fitting the Image of the Absolute Conic through the circular points established by each of these 13 homographies.

Bouguet’s Matlab Toolbox [1] generates a full camera model, with intrinsic calibration parameters as well as the lens distortion model. The lens distortion model is primarily a function of the distance from the principal point, that produces the projections to the image plane that are not equivalent to the ideal pinhole camera model. However, the modeling of the lens distortions allows us to produce rectified images that would be equivalent as those generated by a true pinhole camera. Fig. 9 is the visualization of the lens distortions as provided by the Toolbox. The average angle error was found to be 0.19 degrees.

*E. Error Analysis*

The previous results were obtained by manually selecting the center point of each star in the night sky image, incorporating a possible centroiding error of at most 1 pixel. The angle between two pixels is a function of the camera’s Field of View, and the number of pixels in the image. For this experiment, the angle between two pixels (in the center of the image) is about .021 degrees. However, since the

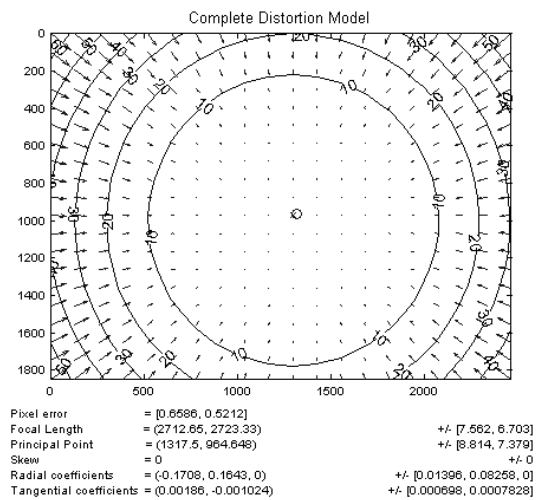


Fig. 9. Visualization of lens distortions as provided by J Bouguet’s Matlab Camera Calibration Toolbox [1].

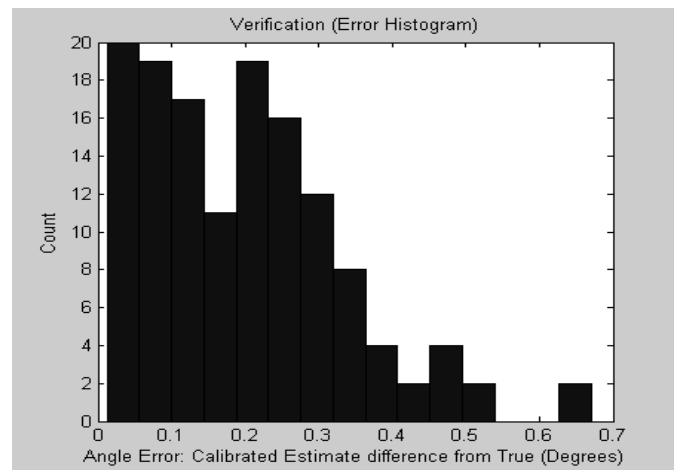


Fig. 10. Error distribution from the difference of true inter-star angles and estimated angles using calibration results from J.Y. Bouguet’s Matlab Camera Calibration Toolbox [1].

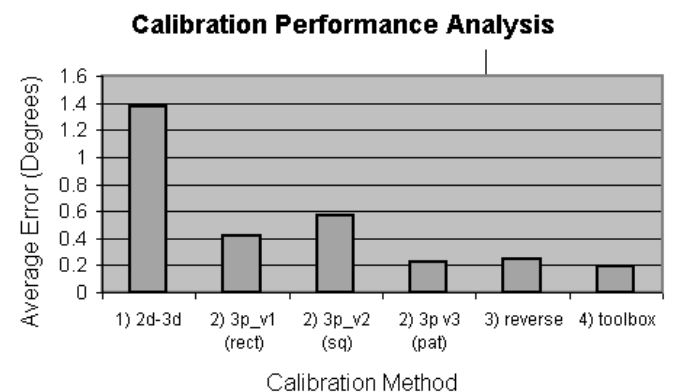


Fig. 11. Summary of average angle error for each calibration technique (without correction for lens distortions)

previous results were obtained without any correction or rectification to compensate for lens distortion, the true error estimate is unknown, even though we obtained highly accurate angle estimates between star pairs. Fig. 11 summarizes the results from the four different calibration techniques without lens distortion rectification.

## V. LENS DISTORTION RECTIFICATION

The difference between the previous results of calibration from section IV and the results from this section, are that the results from this section were obtained by calibration of rectified calibration images. All rectified images (for calibration and for star centroiding) were obtained from the same rectification process provided by Bouguet's camera calibration toolbox for Matlab [1], as illustrated on Fig. 9. The difference between estimated and true Inter-Star angles was computed with lens rectification to analyze the error introduced by lens distortion.

### A. Calibration results from 3 planes (with rectification)

The calibration image (Fig 5b) previously used was rectified to compensate for lens distortions before the new corners of the squares were found. Therefore, new homographies were used to compute the circular points and the Image of the Absolute Conic. With these new calibration parameters, and the new star centroids from the night sky image, we obtained new Inter-Star angle estimates, and compared them against the original true Inter-Star angles. The difference between estimated angles and true angles is shown on Fig. 12, where the average error between star pairs is 0.31 degrees.

The next experiment was to perform the same calibration technique of the 3 planes to the third method previously used where the three planes were on separate images, allowing for a more accurate estimate of the Homographies, and thus, of

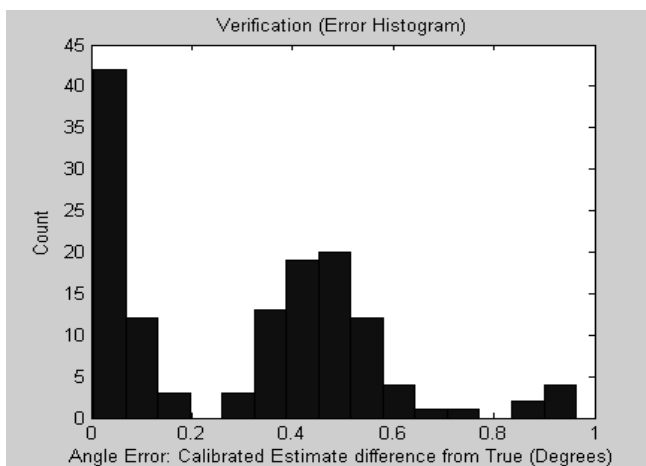


Fig. 12. Error distribution from the difference of true inter-star angles and estimated angles using calibration results from 3 planes (squares) after image rectification of calibration image and night-sky image

the circular points that define the conic. The same image rectification process was applied to the calibration images (Fig. 6) to obtain an average angle error of 0.1233 degrees. Where the histogram of the error between star pairs is shown on Fig. 13.

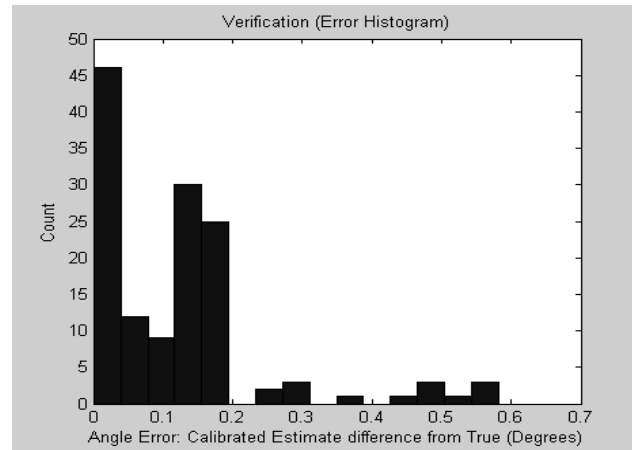


Fig. 13. Error distribution from the difference of true inter-star angles and estimated angles using calibration results from 3 planes (3 separate images) after image rectification of calibration image and night-sky image

### B. Calibration results from Toolbox (with rectification)

Finally, we estimate the Inter-Star angles with the same calibration parameters found earlier (since the calibration from the toolbox included lens distortion compensation) on the new star centroids obtained from the rectified night-sky image. The results are extremely accurate with an average error of 0.0749 degrees between star pairs (with the angle between two pixels is still 0.021 degrees).

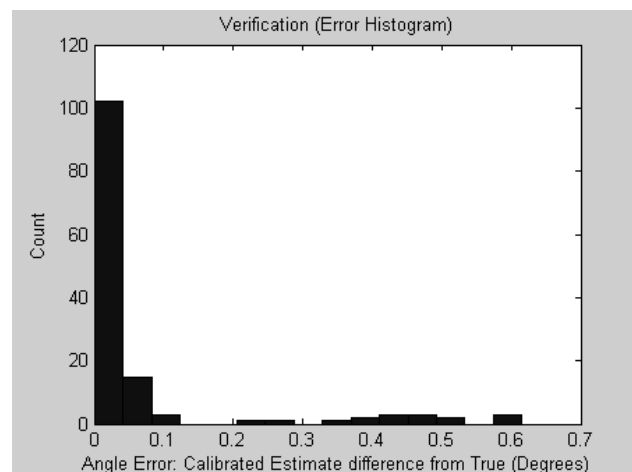


Fig. 14. Error distribution from the difference of true inter-star angles and estimated angles using calibration results Bouguet's Toolbox [1] after image rectification of the night-sky image

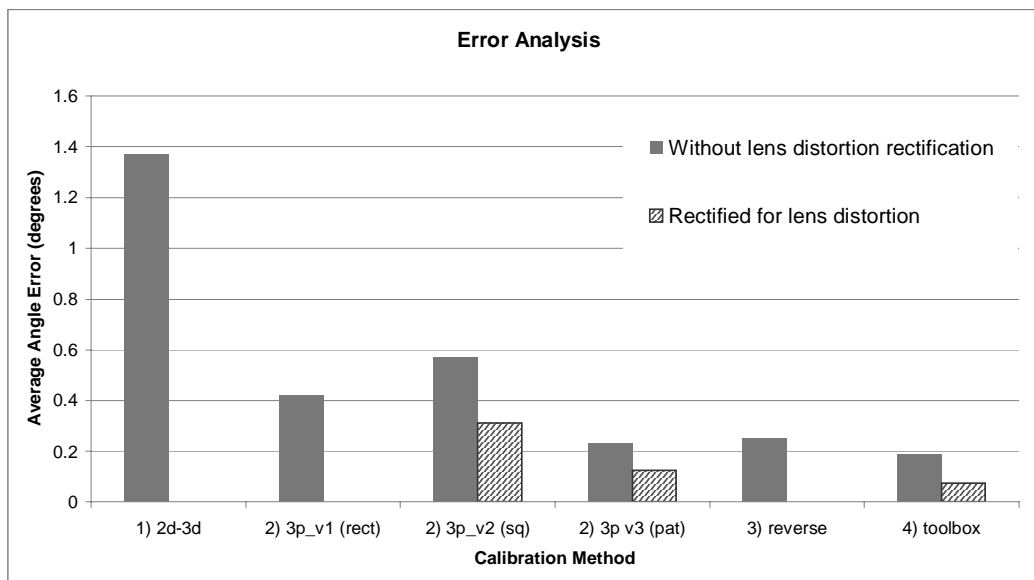


Fig. 15. Camera calibration comparison based on the error between estimated Inter-Star angle and true Inter-Star angle

## VI. CONCLUSIONS

Camera calibration allows for accurate estimates of Inter-Star angle measurements regardless of the camera calibration technique. However, to achieve highly accurate estimates, full calibration must include a lens distortion model in order to properly rectify images to minimize the lens distortion effects. Furthermore, optimum calibration must also incorporate multiple data that allow for optimization of overdetermined solutions.

Our results verify that J. Bouguet's [1] calibration implementation achieve the most accurate angle measurement estimates, however, our basic implementation of Zhang's calibration technique [2] also provides similar highly accurate estimates (although lens distortion rectification was based on Bouguet's toolbox).

Furthermore, our implementation of the reverse calibration technique demonstrated a significant potential for calibrating cameras onboard already deployed spacecrafts, since the error obtained from the estimated angles was comparable to the other calibration techniques.

Inter-Star angle estimates have been demonstrated to be highly accurate (within 0.07 degrees with 0.021 degrees between two pixels), yet further testing must be conducted to minimize the error, possible enhancements to the test procedure include an accurate sub-pixel accurate centroiding algorithm, and increased accuracy can also be achieved by increasing the number of pixels and reducing the field of view.

## APPENDIX

### A. Night-Sky Test Configuration and Data

The camera used all experiments for this study was a Canon SD400 digital camera, with 5 MegaPixels and a focal length of 5.8mm (35mm equivalent of 35mm). The Night sky image used for estimating the inter star angles is shown on Fig. A1, with the corresponding locations of the selected 17 stars. Consequently there are 136 possible unique star pairs, with their inter-star angle ranging from 2 to 34 degrees.



Fig. A1. Night-Sky Image with highlighted star centroid locations.

## ACKNOWLEDGMENT

A special thanks to Dr. Dezhen Song for his critical role as instructor, mentor, advisor, and contributor to this study.

Furthermore, we are also extremely grateful for the contributions and support by Dr. Daniele Mortari, Dr. Igor Carron, Dr. Thomas Talley, and Mr. Charles Hill.

## REFERENCES

- [1] J. Y. Bouguet, "Camera Calibration Toolbox for Matlab" [Online]. Available: [http://www.vision.caltech.edu/bouguetj/calib\\_doc](http://www.vision.caltech.edu/bouguetj/calib_doc)
- [2] Z. Zhang, "A Flexible New Technique for Camera Calibration" *Microsoft Research*, Dec. 1998.
- [3] Bruccoleri, C., Samaan, M.A., Mortari, D., and Junkins, J.L. "Novel Techniques for the Creation of a Uniform Star Catalog" Paper AAS 03-609 of the 2003 AAS/AIAA Astrodynamics Specialist Conference, Big Sky, Montana, August 3-7, 2003
- [4] W.-K. Chen Bauer R., "Distribution of Points on a Sphere with Application to Star Catalogs", *Journal of Guidance and Control*, Vol. 23, No. 1, Jan-Feb 2000.
- [5] Kudva, P., "Flight Star Catalog Development for EOS-AMI", NASA Goddard Space Flight Center Contract NAS5-32590, Task 710-03, TM-421-97-008, March 1997.
- [6] Samaan, M.A., Griffith, T., Junkins, J.L., "Autonomous on-Orbit Calibration Of Star Trackers," 2001 Core Technologies for Space Systems Conference, Colorado Springs, CO, 27-30 Nov. 2001.
- [7] Samaan, M.A., Mortari, and Junkins, L.J. "Non-Dimensional Star Identification for Un-Calibrated Star Cameras," Paper AAS 03-131 of the AAS/AIAA Space Flight Mechanics Meeting. Ponce, Puerto Rico, 9-13 February, 2003.
- [8] Samaan, M.A., Mortari, D., Pollock, T.C., and Junkins, L.J. "Predictive Centroiding for Single and Multiple FOVs Star Trackers," Paper AAS 02-103 presented at the AAS/AIAA Space Flight Mechanics Meeting, San Antonio, TX, 27-31 January, 2002.
- [9] Katake, A., Mortari, D., and Junkins, J.L. "Spacecraft Attitude Estimation using Constrained Re-Centroiding for Star Trackers," *AIAA Journal of Guidance, Control, and Dynamics*.
- [10] Mortari, D., Samaan, M.A., Bruccoleri, C., and Junkins, J.L. "The Pyramid Star Identification Technique," *Navigation*, Vol. 51, No. 3, Fall 2004, pp. 171-183
- [11] Mortari, D., Pollock, T.C., and Junkins, J.L. "Towards the Most Accurate Attitude Determination System Using Star Trackers," *Advances in the Astronautical Sciences*, Vol. 99, Pt. II, pp. 839-850.
- [12] Shalom, E., Alexander, J.W., and Stanton, R.H., "Acquisition and Tracking Algorithms for the ASTROS Star Tracker", Paper AAS 85-050, The Annual Rocky Mountain Guidance and Control Conference, Keystone, CO, 1985.
- [13] Mortari, D., Junkins, J.L., and Samaan, M.A. "Lost-In-Space Pyramid Algorithm for Robust Star Pattern Recognition", Paper AAS 01-004 Guidance and Control Conference, Breckenridge, Colorado, 31 Jan. - 4 Feb. 2001.
- [14] Samaan, M.A., Mortari, D., and Junkins, J.L., "Recursive Mode Star Identification Algorithms", Paper AAS 01-194 Space Flight Mechanics Meeting, Santa Barbara, CA, 11-14 February, 2001.
- [15] A. Klaus, J. Bauer, K. Karner, P. Elbischger, R. Perko, H. Bischof, "Camera Calibration from a Single Night Sky Image," *IEEE Computer Society Conference on Computer Vision and Pattern Recognition*, 2004.
- [16] R. Hartley, A. Zisserman, *Multiple View Geometry in Computer Vision*. Cambridge, 2006, 2<sup>nd</sup> Edition, pp. 153-180.

**Pedro Davalos** obtained his bachelor's degree in computer engineering (2002) and is currently pursuing a masters degree in computer science, both at Texas A&M University, College Station, TX 77843, USA.

Mr. Davalos has worked on various projects as a Research Engineer at the Spacecraft Technology Center since 2002 (College Station, TX). Previous positions also include Senior Video Network Specialist at the Educational Broadcast Services Department of Texas A&M. Where his research interests include signal processing, machine learning, robotics, and computer vision. Mr. Davalos is also a member of the American Institute of Aeronautics and Astronautics.